2D Materials

PAPER

Crack-assisted, localized deformation of van der Waals materials for enhanced strain confinement

To cite this article: Juyoung Leem *et al* 2019 *2D Mater.* **6** 044001

View the article online for updates and enhancements.

This content was downloaded from IP address 192.17.15.212 on 24/07/2019 at 16:31

2D Materials

PAPER

RECEIVED
1 February 2019

REVISED
25 June 2019

ACCEPTED FOR PUBLICATION
3 July 2019

PUBLISHED
24 July 2019

Crack-assisted, localized deformation of van der Waals materials for enhanced strain confinement

Juyoung Leem[1], Yeageun Lee[1], Michael Cai Wang[1,5], Jin Myung Kim[2], Jihun Mun[3], Md Farhadul Haque[1], Sang-Woo Kang[3,4,6] and SungWoo Nam[1,2,6]

[1] Department of Mechanical Science and Engineering, University of Illinois at Urbana-Champaign, Urbana, IL 61801, United States of America
[2] Department of Materials Science and Engineering, University of Illinois at Urbana-Champaign, Urbana, IL 61801, United States of America
[3] Advanced Instrumentation Institute, Korea Research Institute of Standards and Science, Daejeon 34113, Republic of Korea
[4] Science of Measurement, University of Science and Technology, Daejeon 34113, Republic of Korea
[5] Current affiliation: Department of Mechanical Engineering, University of South Florida, Tampa, FL 33620, United States of America
[6] Authors to whom any correspondence should be addressed.

E-mail: swkang@kriss.re.kr and swnam@illinois.edu

Keywords: crack-lithography, crumpling, 2D materials, strain engineering

Supplementary material for this article is available online

Abstract

The crumpling of two-dimensional (2D) materials is one of the most widely used ways to create three-dimensional (3D) out-of-plane structures from 2D materials and to apply in-plane strain for strain-induced material property modulation. Although the elastic compressive strain induced crumpling of 2D materials is a simple and versatile way to form 3D structures, the resulting structures are rather simple where crumples are formed in a delocalized manner. Here, we report a new approach inspired by crack lithography to localize deformation and achieve localized crumpling of 2D materials. As a result, a mixed-dimensional structure composed of flat (2D) and crumpled (3D) structure is formed monolithically in 2D materials. We present structural analysis of our mixed-dimensional structure of graphene, where the localized prestrain was amplified to be 330% of the macroscale prestrain. In addition, we demonstrate the material densification and the strain localizations of our mixed-dimensional structure of monolayer MoS_2 and graphene based on Raman and photoluminescence spectral characterizations. Finally, our mixed-dimensional graphene structure is fabricated into a stretchable strain sensor, where it exhibits four times enhanced gauge factor compared to that of delocalized crumpled graphene.

Introduction

Deformation of two-dimensional (2D) materials has been widely investigated to introduce three-dimensionality (3D) to 2D materials and to modulate their material properties in extrinsic ways by applying mechanical strains [1, 2]. One of the widely used deformation strategies is the 'crumpling' of 2D materials, which utilizes elastic compressive strains to form out-of-plane buckle-delaminated structure of a 2D material [3–6]. Structural characteristics, such as height (or amplitude) and wavelength of crumpled structures, are mainly controlled by substrate prestrains, which had been applied to the substrate prior to a 2D material transfer. These crumpled 2D materials exhibit enhanced light–matter interactions [5, 7], increased piezoresistivity with higher stretchability [8, 9], and tuneable wettability [3, 10]. However, the crumpling method produces relatively simple, delocalized crumple structures, where crumples are formed everywhere in 2D materials. Although there have been various efforts to impart higher complexity in wrinkled 2D material structures [11], the fabrication process requires a special patterning process, and the substrate material restricts the stretchability of the resulting structures.

Crack lithography is an unconventional patterning technique to form patterns via material failures, and it has been demonstrated as a time- and cost-effective approach with high throughput [12]. Various external forces, such as optical [13], thermal [14, 15], electrical [16], and mechanical forces [17] or combined forces

© 2019 IOP Publishing Ltd

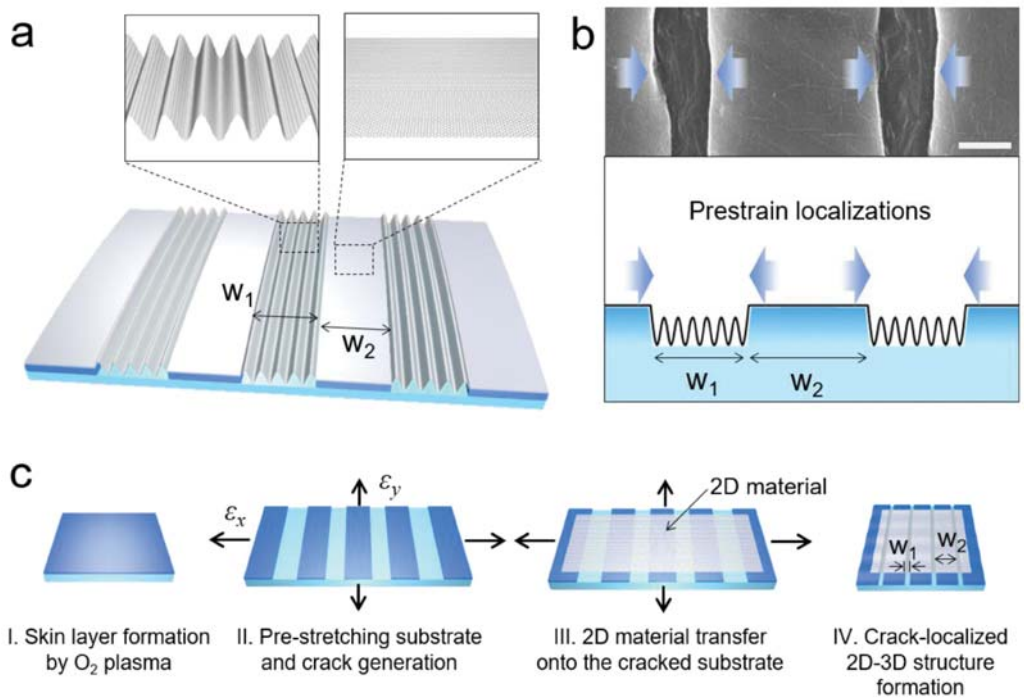

Figure 1. Configuration of the crack-assisted 2D–3D mixed-dimensional structures and fabrication process. (a) Schematic illustration of monolithically formed flat (2D)—crumpled (3D) structure. The width of crumpled region is W_1, and the width of flat region is W_2. (b) SEM image of the 2D–3D mixed-dimensional structure and a schematic illustration describing prestrain localizations. Scale bar is 500 nm. (c) Fabrication process of the crack-assisted 2D–3D mixed-dimensional structure.

[18], can be used to apply tensile stress and introduce cracks in materials. Among them, mechanical force induced crack formation has advantages in its fabrication process, for example, the rapid process [19] and the controllable structures with applied mechanical strain control [20]. This crack-assisted patterning strategy via mechanical forces can be easily combined with the 2D material crumpling method since mechanical deformation of a substrate is utilized in both strategies.

In this paper, we report a simple method to localize crumples in specific portions of a 2D material surface by localizing applied prestrains, while other portions of the 2D material surface remain flat. We realized the localized crumples of 2D materials on an elastomeric substrate with a stiff skin layer on top. The skin layer fractured with applied prestrains forms crack-assisted patterns. The crack-assisted pattern width was tuneable with the surface treatment time to form a skin layer. Furthermore, the applied prestrains were localized at openings between two cracked patterns because the patterns of the stiffer skin layer stretch much less than the original soft substrate under the skin layer does. The localized prestrain at the crumpled region is also amplified, and it was estimated to be 1000%, which is 3.3 times the macroscale prestrain. The strain localization effect is characterized with Raman spectrum mapping of graphene 2D–3D mixed-dimensional structure and with photoluminescence (PL) mapping of monolayer MoS_2 2D–3D structure. Finally, the graphene 2D–3D structure was fabricated into a strain sensor, and its gauge factor was 4 times higher than delocalized crumpled graphene, which is originated from prestrain localization and amplification.

Results and discussion

Figure 1 illustrates the unique configuration and the fabrication process of crack-assisted mixed-dimensional structure of 2D materials. Figures 1(a) and (b) show schematic illustrations and a scanning electron microscope (SEM) image of our 2D–3D structure. On a crack-patterned substrate, a 2D material (graphene in this image) formed into out-of-plane crumpled structures in W_1 regions and remained to be flat in W_2 regions. Our continuous flat (2D) and crumpled (3D) structure of 2D material is unique because applied prestrain is localized at the W_1 regions where we can achieve localized crumples formation with higher prestrains than the applied macroscale prestrain.

The fabrication process of the crack-assisted 2D–3D mixed-dimensional structures with localized and amplified prestrain is shown in figure 1(c). First, we treated an elastomeric substrate (3M™ VHB™) with oxygen (O_2) plasma to form a stiff skin layer (figure 1(c)-(I)). The thickness of the skin layer was controlled by the plasma treatment time. We then stretched the elastomeric substrate with a skin layer to form crack patterns on the elastomeric substrate (figure 1(c)-

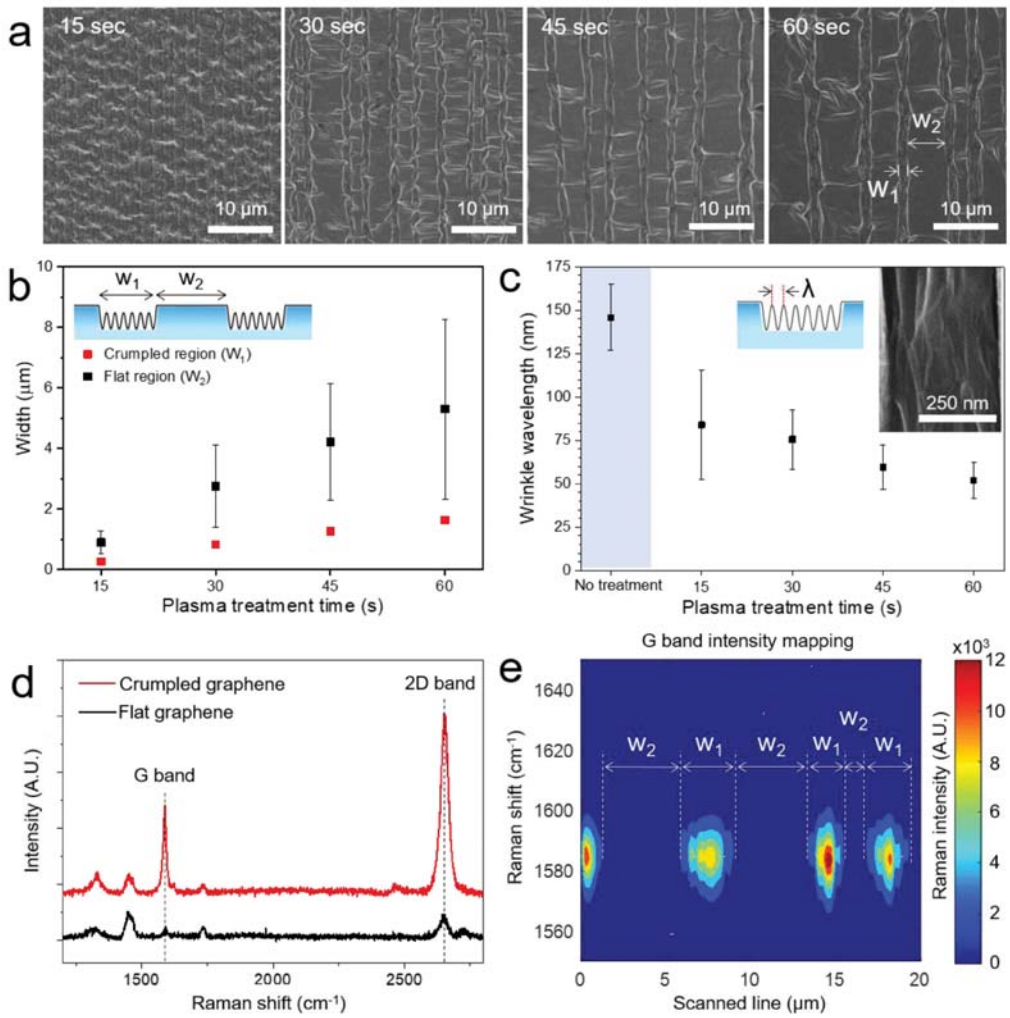

Figure 2. Structural controllability and strain localization and amplification effect of the crack-assisted 2D–3D mixed-dimensional structure. (a) SEM images of the crack-assisted 2D–3D structures of graphene prepared with different plasma treatment times. (b) Structural controllability of W_1 and W_2 in graphene 2D–3D structures by modulating plasma treatment time. (c) Wrinkle wavelength (λ) analysis of graphene crumples in W_1 regions as well as delocalized crumpled graphene sample (marked as 'No treatment' in the plot). (d) Raman spectra of crumpled and flat graphene from the 2D–3D mixed-dimensional graphene structure. (e) Graphene G peak intensity mapping of a Raman line scanning across the 2D–3D mixed-dimensional graphene.

(II)). We used macroscale prestrains of 300% in x-axis and 30% in y-axis, and the cracks were formed along y-axis owing to fracturing of the skin layer by x-axis stretching. The relatively small amount of prestrain in y-axis (ε_y) induced the micrometre-scale undulating topography observed at the surface of flat regions (W_2) when ε_y is released, and the undulating topography became flatter with decreasing ε_y (figure S1 (stacks.iop.org/TDM/6/044001/mmedia)). We applied a relatively small amount of prestrain in the y-axis to avoid potential fracture due to unintended tensile stress in y-axis during handling. Since the stiffer skin layer is less stretchable than the elastomeric substrate, the skin layer was barely stretched during this stretching step and most of stretching occurred at the freshly exposed elastomeric substrate. While the substrate was stretched with the applied prestrains, a 2D material (graphene in this image) was transferred onto the stretched substrate (figure 1(c)-(III)). Once the transfer process was completed, prestrains applied in both x- and y-axes were gently removed to form the mixed-dimensional structure of 2D materials (figure 1(c)-(IV)). This mechanical property change due to plasma treatment enables us to create patterns on the elastomeric substrate with crack lithography technique (figures 1(c)-(II) and S2) and to localize crumpled structures of 2D materials only in W_1 area, by localizing applied prestrain (figures 1(c)-(III and IV)).

To demonstrate our capability to control widths of W_1 and W_2, and wrinkle wavelength of the localized crumples, we analysed our mixed-dimensional structures prepared with different plasma treatment times. The crumpled region width (W_1) and flat region width (W_2) become wider as the plasma treatment time on the substrate becomes longer (figure 2(a)) because the longer plasma time induces the thicker skin layer

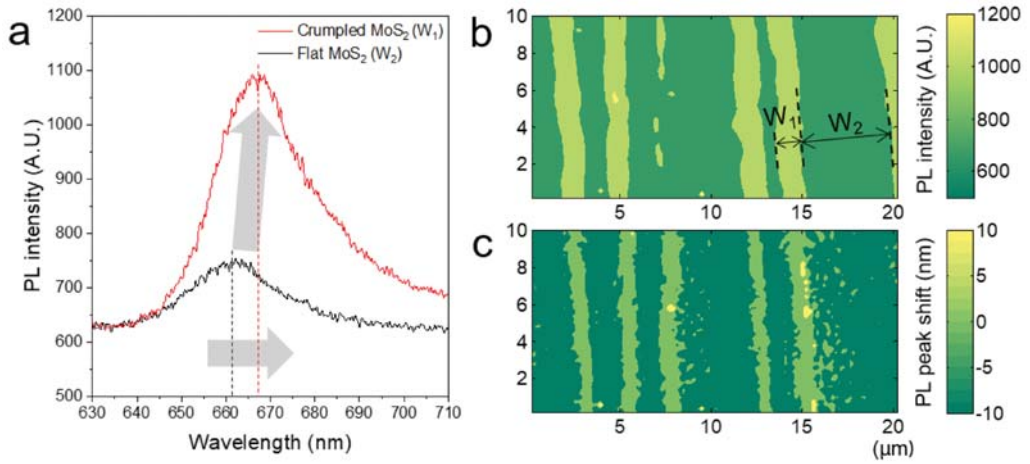

Figure 3. PL spectroscopy of MoS_2 2D–3D mixed-dimensional structure. (a) MoS_2 A exciton PL spectra from two point: a point from crumpled region (W_1) and a point from flat region (W_2). A exciton peak of crumpled region was red-shifted, which implies the material is under tension, and the intensity of the peak is enhanced. (b) and (c) PL areal mapping of 20 μm by 10 μm window: (b) intensity mapping of the peak and (c) peak wavelength shift mapping.

(figure S2). We further investigated W_1 and W_2 regions shown in figure 2(a) with atomic force microscope (AFM) as well as tilted view SEM images to present mixed dimensionality of the fabricated structure (figures S3 and S4). A statistical analysis on W_1 and W_2 was conducted by measuring widths from multiple SEM images to characterize our structure quantitatively (figure 2(b)). We observed that the average values of W_1 and W_2 linearly increased with increasing plasma treatment time, whereas the ratio between them, $R_w = W_2/W_1$, remained to be almost constant ($R_{w,15s} = 3.33$, $R_{w,30\ s} = 3.31$, $R_{w,45\ s} = 3.35$, $R_{w,60\ s} = 3.23$). In addition, we estimated amplified prestrain at the crumpled region (W_1), and it was approximately 3.3 times larger than the applied macroscale prestrain when R_w is 3.3 (see supplementary information section 2 for more discussion).

We further demonstrate that the localized strain at W_1 determines wavelength (λ) of the crumples (figure 2(c), representative SEM images of each case are shown in figure S5). As a control sample, we prepared uniaxially crumpled graphene with same prestrains of 300% (in x-axis) by 30% (in y-axis) without plasma treatment on the substrate. The average wavelength of uniaxially crumpled graphene on an elastomeric substrate without plasma treatment ($\lambda_{\text{no treatment}}$) was estimated to be 146 nm $\pm$ 19nm ($\pm$1-standard deviation). On the other hand, average wavelength values of crumpled graphene at crumpled region (W_1 region) prepared with different plasma times were estimated to be much smaller than $\lambda_{\text{no treatment}}$. Specifically, the structure fabricated on 15 s plasma treated substrate showed the largest wavelength ($\lambda_{15\ s}$) among the four plasma treatment cases. $\lambda_{15\ s}$ was 83.9 nm $\pm$ 31.5 nm (about 57% of $\lambda_{\text{no plasma}}$). The smallest wavelength case was $\lambda_{60\ s}$, and it was 51.9 nm $\pm$ 10.6 nm (about 36% of $\lambda_{\text{no plasma}}$), implying larger localized prestrain compared to other cases. Since the crumpling of graphene in our samples occurred under extremely high compression, we assume that the crumpled structure is well developed over the area such that the larger prestrain does not create additional number of winkles but does induce geometrical deformations [21]. The amplified prestrain at W_1 regions was estimated to be as high as 1000% (see supplementary information section 4 for more discussion).

To characterize the prestrain localization in W_1 region of our mixed-dimensional graphene structures, we carried out Raman characterizations. Raman spectroscopy on the crack-assisted 2D–3D graphene structures clearly shows the localized deformation of our mixed-dimensional graphene (figures 2(d) and (e)). Raman spectra were collected from two points, one from W_1 and the other from W_2. Both spectra show two distinct characteristic peaks of graphene: G and 2D bands [22]. Raman intensity from crumpled region (W_1) was larger than the one from flat region (W_2), implying material is densified at the W_1 region due to localized crumples. A line scan of Raman spectra clearly shows periodic intensity change over the graphene 2D–3D mixed-dimensional structure (figures 2(e) and S6).

We further expanded our approach to 2D transition metal dichalcogenide (TMDC) monolayer, i.e. monolayer MoS_2 synthesized by metal organic chemical vapour deposition (MOCVD). PL spectra of semiconductor materials are also sensitive to applied in-plane strains owing to strain-induced bandgap modulation [23–26]. A 2D semiconducting material, monolayer MoS_2 was used to form crack-assisted 2D–3D mixed-dimensional structures. We took PL spectra from a point in W_1 region and a point in W_2 region to compare the intensity and A exciton peak position of monolayer MoS_2 (figure 3(a)). The centre of A exciton PL peak from a crumpled MoS_2 region was red-shifted with respect to the centre of PL peak from a flat

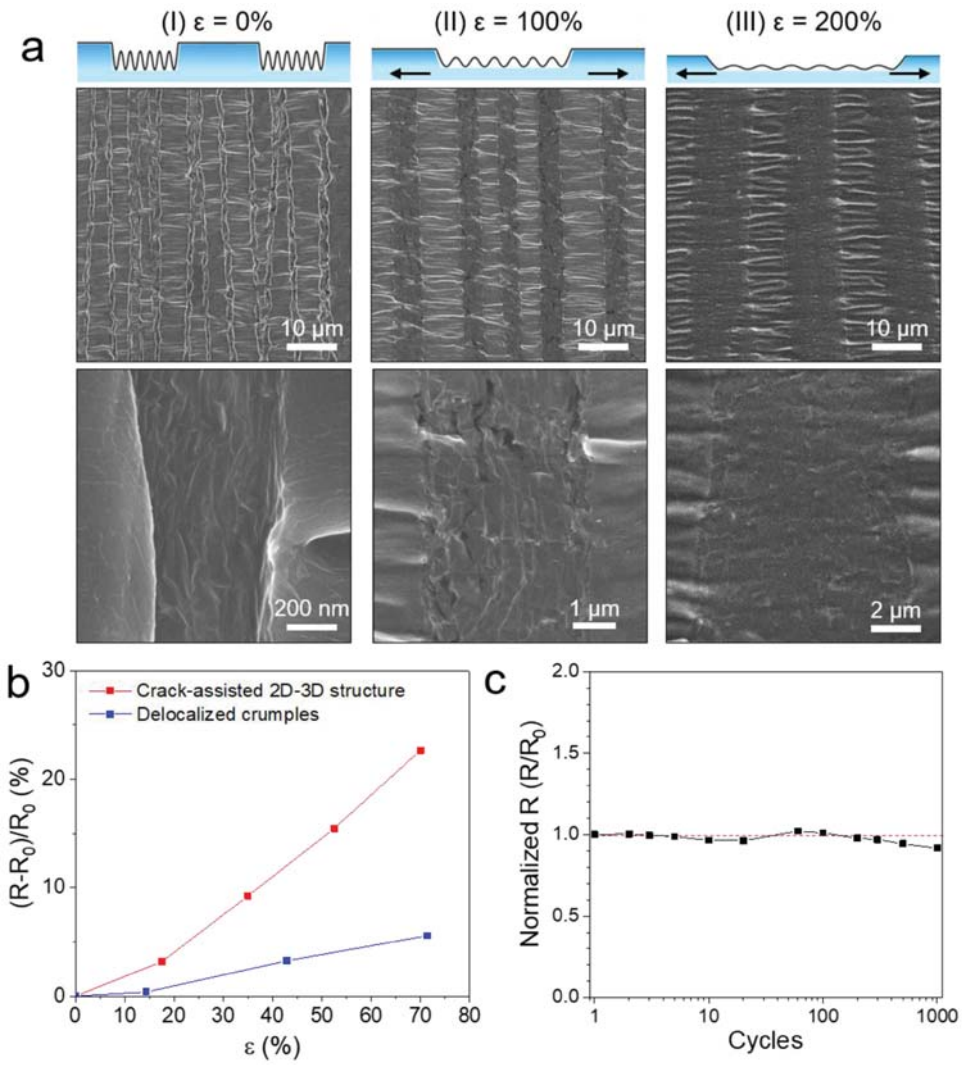

Figure 4. Mechanical stretchability and strain sensor demonstration. (a) Schematic illustrations and SEM images of our crack-assisted 2D–3D structures under different tensile strain: (I) $\varepsilon = 0\%$, (II) $\varepsilon = 100\%$, and (III) $\varepsilon = 200\%$. This highly stretchable 2D–3D mixed-dimensional graphene was fabricated into a strain sensor, and the sensor showed (b) enhanced piezoresistivity owing to amplified prestrain at localized crumples, and (c) mechanical robustness over 1000 cycles.

MoS_2 region, which implies MoS_2 in crumpled region is under tensile stress. The tensile strain estimated in the crumpled region (W_1) was approximately 0.27% [24]–0.38% [25]. The peak intensity was higher in the spectrum from crumpled region, owing to the material densification as well as the exciton funnelling effect [27].

Furthermore, we performed PL 2D mapping to show continuous spectral change in 2D–3D MoS_2 structures. Figure 3(b) shows maximum intensity mapping over a 20 μm by 10 μm window. As we discussed in figure 3(a), crumpled region (W_1) exhibits higher PL intensity, which is clearly shown in our 2D mapping results (figure 3(b)). PL peak shift in MoS_2 2D–3D structures was also observed in PL 2D mapping (figure 3(c)). The peak shift ($\Delta\lambda$) was calculated based on measured PL wavelength from each point and the average PL wavelength over flat the area ($\Delta\lambda = \lambda - \lambda_{avg}$). We observed red-shift in the crumpled region (W_1) with respect to the flat region (W_2), which implies the crumpled MoS_2 structure is under tension, consistent with the PL analysis in figure 3(a).

Finally, we carried out systematic studies of mechanical stretchability of our mixed-dimensional graphene structures. We prepared a crack-assisted 2D–3D mixed-dimensional structure with prestrains of 300% (in x-axis) and 30% (in y-axis) and investigated the morphology change under different tensile strains (e.g. 0%, 100%, and 200%) with SEM imaging (figure 4(a)). Similar to previously reported crumpled graphene structures [5, 28, 29], we found that our crack-assisted 2D–3D structure is also mechanically stretchable. Specifically, crumpled graphene structures in crumpled region (W_1) became flatter with increasing tensile strain. On the other hand, undulating structures in flat region (W_2), which formed along

the x-axis in the SEM images, became more obvious because the substrate contracted in the transverse direction (along y-axis) due to the Poisson effect.

The mechanical stretchability and the localized, amplified prestrain in our crack-assisted 2D–3D structures enables our structure to exhibit enhanced piezoresistivity for strain sensors. We fabricated the graphene 2D–3D structure-based strain sensor and measured its resistance over tensile strain of 70% (figure 4(b)). As a control device, a delocalized crumpled graphene prepared with the same prestrains was also fabricated into a strain sensor. Gauge factor ($G_f = \Delta R_N/\Delta\varepsilon$, where $\Delta R_N = \Delta R/R_0 = (R - R_0)/R_0$, R_0 is resistance at 0%, and ε is applied strain), which is also the slope of line plots shown in figure 4(b), of 2D–3D graphene structure was approximately 4 times larger than that of delocalized crumpled graphene. Specifically, G_f of 2D–3D mixed-dimensional graphene was 0.33, and G_f of delocalized crumpled graphene was 0.082. We attribute the increased gauge factor to the strain amplification at W_1 regions for enhanced piezoresistivity. We believe our approach can be combined with existing approaches, such as using heterostructures [30], to achieve even higher gauge factor.

We also characterized mechanical robustness of our 2D–3D mixed-dimensional graphene-based strain sensor (figure 4(c)). As our device was mechanically stretched and released, we monitored its electrical resistance up to 1000 cycles and compared with initial resistance prior to any stretching. Our results showed that the electrical resistance of the graphene 2D–3D structure remains minimally changed up to 1000 cycles of stretching and releasing, implying negligible structural/material failure during the cycles.

Our results clearly showed that the synergistic combination of crack lithography and crumpling of 2D materials is a simple and versatile approach to achieve 2D–3D mixed-dimensional 2D materials with localized and amplified prestrains. We believe there are three unique aspects of our work. First, we demonstrate the new concept of "2D–3D mixed-dimensional structures" which are created through the unconventional strategy—combination of crack lithography and the crumpling method. This strategy suggests a simple but versatile way to form mixed-dimensional structures, which possess higher structural complexity compared to structures prepared solely with either crack-lithography or crumpling method. Second, we successfully demonstrate our new approach enables localizing and amplifying the applied prestrain at selected portions of the 2D materials (W_1 regions). The localized and amplified prestrains crumple a 2D material only at selective W_1 regions, with 3.3 times of applied macroscale prestrain, and locally modulate the material functionality of the deformed 2D material, such as piezoresistivity enhancement. Finally, the high mechanical stretchability with improved strain localization of the 2D–3D mixed-dimensional structure also makes our structure a promising candidate for flexible and stretchable electronic devices.

Conclusions

In this paper, we demonstrate the crack-assisted 2D–3D mixed-dimensional structure formation of 2D materials for localization of crumpled structure. Our fabricated structure forms a monolithic structure of flat (2D) and crumpled (3D) 2D materials without a conventional lithography process, and the amplification and localization of prestrain were demonstrated through structural and spectroscopic characterizations. The localized prestrain in a crumpled 2D material region was 3.3 times higher than the applied prestrain. Specifically, an applied macroscale prestrain of 300% leads to a local prestrain of 1000%. Furthermore, the mechanical stretchability and robustness of our 2D–3D structure were demonstrated with approximately 4 times higher gauge factor when configured as a strain sensor. We believe our new approach opens up a new possibility in research field of 2D strain engineering and mechanical self-assembly by enabling localized crumples and amplified strain.

Materials and methods

Graphene synthesis

Graphene samples were synthesized in a low-pressure chemical vapour deposition (CVD) system (Rocky Mountain Vacuum Tech Inc., CO). Copper foil was purchased from MTI (EQ-bccf-25u, MTI corp., CA) and cut into 4 inches by 2.5 inches piece for synthesis. A copper foil was pretreated by submerging into a bath of acetic acid (Sigma-Aldrich, MA) for 10 min to gently remove surface oxides on the copper foil. The pretreated copper foil was then inserted into the quartz tube of the CVD system, and the system was heated up to 1035 °C in 45 min under low pressure (150 mTorr) and hydrogen atmosphere, followed by annealing process for an hour at 1035 °C. Then graphene growth was started with adjusting pressure to 520 mTorr and introducing methane (CH_4) gas with a flow rate ratio of 2:1 between methane and hydrogen. The growth time was 5 min, and the growth was finished with turning off hydrogen and methane gases and electric heater, turning on argon gas line, and reducing pressure to 330 mTorr. CVD system was cooled down to room temperature.

Graphene transfer

Unwanted graphene on the backside of copper foil was removed by oxygen plasma before graphene transfer. Poly(methyl methacrylate) (PMMA C6, MicroChem, MA) was spin-coated onto the top graphene to protect the graphene from oxygen plasma. The PMMA/

graphene/copper foil was flipped, and backside graphene was etched by oxygen plasma. PMMA layer was removed by submerging in an acetone bath for 5 min. Then graphene/copper foil was cut into 3 cm by 1 cm pieces. Meanwhile, an elastomeric substrate (3M™ VHB™ 4910, 3M, MN) was plasma treated at low pressure, 0.2 mbar, under oxygen atmosphere (Nano plasma system, Diener Electronic GmbH, Germany) to form skin layer. The plasma power was 500 W, and duration of surface treatment was controlled, from 15 s to 60 s. The plasma treated VHB substrate was pre-stretched with our custom-built stretcher setup. After the substrate prestretching, the graphene/copper foil piece was gently put onto the prestretched elastomeric substrate with a skin layer keeping the graphene facing the substrate. A drop of an aqueous solution of sodium persulfate ($Na_2S_2O_8$, Sigma-Aldrich, MA) was applied onto copper foil, and the puddle of solution was kept larger than the copper foil. Once the copper foil was completely etched by the solution, the solution was removed and replaced with deionized (DI) water. The DI water puddle was replaced with fresh DI water 2–3 times for rinsing purpose. After the last rinsing with DI water, prestrains applied to the substrate were carefully removed, and we let the sample rest for few hours to restore the substrate's original size.

MoS_2 synthesis and transfer

MoS_2 samples used in this paper were single layer MoS_2 grown by metal organic chemical vapor deposition (MOCVD) at relatively low temperature [31–33] on a SiO_2/Si substrate. The MoS_2/SiO_2/Si sample was gently put onto a prestretched elastomeric substrate with a skin layer, keeping the MoS_2 facing the substrate. A DI water droplet was applied onto the Si/SiO_2/MoS_2, and the penetration of DI water between MoS_2 and SiO_2 allowed the delamination and transfer of MoS_2 onto the elastomeric substrate. DI water was removed from the puddle, and SiO_2/Si was carefully removed. Prestrains applied to the substrate were carefully removed, and we allow the sample rest for few hours to restore the substrate's original size.

Crack-assisted structural analysis: crack width and height analysis (figure S2)

The crack width and height of crack-patterned elastomeric substrate with a stiff skin layer were analysed based on AFM (MFP-3D, Asylum Research, CA) height profiles. Same AFM system was used to scan W_1 and W_2 regions shown in figure S3.

Crack-assisted structural analysis: W_1 and W_2 analysis (figure 2)

The crumpled region width (W_1) and the flat region width (W_2) were analysed based on SEM (Hitachi S-4800, Hitachi, Japan) images. Same SEM system was used for the rest of SEM images presented in this work.

2D material wrinkle wavelength in crumpled region (W_1) analysis (figures 2 and S5)

Crack-assisted 2D–3D structures of graphene were fabricated with four different plasma treatment times, i.e. 15, 30, 45, and 60 s, and the wrinkle wavelength analysis was conducted using SEM images of those samples.

Raman spectroscopy (figures 2, S6 and S7)

Renishaw Raman/PL system (Renishaw, UK) was used for Raman spectroscopy. Point measurements (figures 2(d) and S7) were performed on randomly selected points in flat region and crumpled region with 630 nm wavelength and exposure time of 30 s. Laser spot size of the system is 1.5 μm. Line scan (figures 2(e) and S6) of Raman spectroscopy was conducted over 20 μm length with 0.25 μm step size.

PL measurement (figure 3)

NanoPhoton Raman/PL system (NanoPhoton Raman 11, Japan) was used for PL mapping. The excitation source was a 532 nm laser, and the excitation power was 20 μW to prevent thermal damage to MoS_2 and the polymer substrate. The line-shape illumination with step size of 0.2 μm and exposure time of 5 s were used for fast PL areal mapping.

Strain sensor fabrication and characterization

A uniaxially crumpled graphene on a VHB substrate and a crack-assisted 2D–3D structure sample were fabricated with prestrains of 300% and 100%. Each sample was re-stretched with strains of 200% and 50%, and a shadow mask was used to cover the middle portion of the graphene. 40 nm-thick Au was deposited onto each sample by thermal evaporator (Nano 36, Kurt J. Lesker, PA) to form electrodes. At each electrode, a thin copper foil was attached with a conductive silver paint (Ted Pella). A strain sensor device was connected to a sourcemeter (Keithley 2614B, Keithley, OH), and voltage-current was measured over the voltage range of −1V to 1V.

Acknowledgments

This work was supported by NSF (MRSEC DMR-1720633 and CMMI-1554019), NASA (ECF NNX16AR56G), ONR (YIP N00014-17-1-2830), AFOSR (FA2386-17-1-4071 and FA9550-16-1-0251) and KRISS (KRISS–2018–GP2018-0012). Material preparation and characterizations were carried out in the Micro and NanoTechnology Laboratory, as well as in the Materials Research Laboratory Central Research Facilities at University of Illinois at Urbana-Champaign. This research was primarily supported by the NSF through the University of Illinois at Urbana-Champaign Materials Research Science and Engineering Center DMR-1720633.

Conflict of interest

The authors declare that they have no conflict of interest.

ORCID iDs

Juyoung Leem https://orcid.org/0000-0002-0690-7784
Michael Cai Wang https://orcid.org/0000-0003-3300-852X
Sang-Woo Kang https://orcid.org/0000-0001-5245-0300
SungWoo Nam https://orcid.org/0000-0002-9719-7203

References

[1] Wang M C, Leem J, Kang P, Choi J, Knapp P, Yong K and Nam S 2017 Mechanical instability driven self-assembly and architecturing of 2D materials *2D Mater.* **4** 022002
[2] Chen P-Y, Liu M, Wang Z, Hurt R H and Wong I Y 2017 From flatland to spaceland: higher dimensional patterning with two-dimensional materials *Adv. Mater.* **29** 1605096
[3] Zang J, Ryu S, Pugno N, Wang Q, Tu Q, Buehler M J and Zhao X 2013 Multifunctionality and control of the crumpling and unfolding of large-area graphene *Nat. Mater.* **12** 321–5
[4] Wang M C, Chun S, Han R S, Ashraf A, Kang P and Nam S 2015 Heterogeneous, three-dimensional texturing of graphene *Nano Lett.* **15** 1829–35
[5] Kang P, Wang M C, Knapp P M and Nam S 2016 Crumpled graphene photodetector with enhanced, strain-tunable, and wavelength-selective photoresponsivity *Adv. Mater.* **28** 4639–45
[6] Chen P-Y, Sodhi J, Qiu Y, Valentin T M, Steinberg R S, Wang Z, Hurt R H and Wong I Y 2016 Multiscale graphene topographies programmed by sequential mechanical deformation *Adv. Mater.* **28** 3564–71
[7] Kang P, Kim K-H, Park H-G and Nam S 2018 Mechanically reconfigurable architectured graphene for tunable plasmonic resonances *Light Sci. Appl.* **7** 17
[8] Kim K S, Zhao Y, Jang H, Lee S Y, Kim J M, Kim K S, Ahn J-H, Kim P, Choi J-Y and Hong B H 2009 Large-scale pattern growth of graphene films for stretchable transparent electrodes *Nature* **457** 706–10
[9] Wang Y, Yang R, Shi Z, Zhang L, Shi D, Wang E and Zhang G 2011 Super-elastic graphene ripples for flexible strain sensors *ACS Nano* **5** 3645–50
[10] Choi J, Mun J, Wang M C, Ashraf A, Kang S-W and Nam S 2017 Hierarchical, dual-scale structures of atomically thin MoS_2 for tunable wetting *Nano Lett.* **17** 1756–61
[11] Lee W-K, Kang J, Chen K-S, Engel C J, Jung W-B, Rhee D, Hersam M C and Odom T W 2016 Multiscale, hierarchical patterning of graphene by conformal wrinkling *Nano Lett.* **16** 7121–7
[12] Kim M, Kim D-J, Ha D and Kim T 2016 Cracking-assisted fabrication of nanoscale patterns for micro/nanotechnological applications *Nanoscale* **8** 9461–79
[13] Mirkhalaf M, Dastjerdi A K and Barthelat F 2014 Overcoming the brittleness of glass through bio-inspiration and micro-architecture *Nat. Commun.* **5** 3166
[14] Nam K H, Park I H and Ko S H 2012 Patterning by controlled cracking *Nature* **485** 221–4
[15] Xia Z C and Hutchinson J W 2000 Crack patterns in thin films *J. Mech. Phys. Solids* **48** 1107–31
[16] Sircar S, Choudhury M D, Karmakar S, Tarafdar S and Dutta T 2018 Crack patterns in drying laponite–NaCl suspension: role of the substrate and a static electric field *Langmuir* **34** 6502–10
[17] Li Z, Zhai Y, Wang Y, Wendland G M, Yin X and Xiao J 2017 Harnessing surface wrinkling-cracking patterns for tunable optical transmittance *Adv. Opt. Mater.* **5** 1700425
[18] Seghir R and Arscott S 2015 Controlled mud-crack patterning and self-organized cracking of polydimethylsiloxane elastomer surfaces *Sci. Rep.* **5** 14787
[19] Zhu X, Mills K L, Peters P R, Bahng J H, Liu E H, Shim J, Naruse K, Csete M E, Thouless M D and Takayama S 2005 Fabrication of reconfigurable protein matrices by cracking *Nat. Mater.* **4** 403–6
[20] Huang J, Kim B C, Takayama S and Thouless M D 2014 The control of crack arrays in thin films *J. Mater. Sci.* **49** 255–68
[21] Zhang Q and Yin J 2018 Spontaneous buckling-driven periodic delamination of thin films on soft substrates under large compression *J. Mech. Phys. Solids* **118** 40–57
[22] Ferrari A C *et al* 2006 Raman spectrum of graphene and graphene layers *Phys. Rev. Lett.* **97** 187401
[23] Johari P and Shenoy V B 2012 Tuning the electronic properties of semiconducting transition metal dichalcogenides by applying mechanical strains *ACS Nano* **6** 5449–56
[24] He K, Poole C, Mak K F and Shan J 2013 Experimental demonstration of continuous electronic structure tuning via strain in atomically thin MoS_2 *Nano Lett.* **13** 2931–6
[25] Conley H J, Wang B, Ziegler J I, Haglund R F, Pantelides S T and Bolotin K I 2013 Bandgap engineering of strained monolayer and bilayer MoS_2 *Nano Lett.* **13** 3626–30
[26] Li H *et al* 2015 Optoelectronic crystal of artificial atoms in strain-textured molybdenum disulphide *Nat. Commun.* **6** 7381
[27] Castellanos-Gomez A, Roldán R, Cappelluti E, Buscema M, Guinea F, van der Zant H S J and Steele G A 2013 Local strain engineering in atomically thin MoS_2 *Nano Lett.* **13** 5361–6
[28] Yong K, Ashraf A, Kang P and Nam S 2016 Rapid stencil mask fabrication enabled one-step polymer-free graphene patterning and direct transfer for flexible graphene devices *Sci. Rep.* **6** 24890
[29] Kim M, Kang P, Leem J and Nam S 2017 A stretchable crumpled graphene photodetector with plasmonically enhanced photoresponsivity *Nanoscale* **9** 4058–65
[30] Kim S, Dong Y, Hossain M M, Gorman S, Towfeeq I, Gajula D, Childress A, Rao A M and Koley G 2019 Piezoresistive graphene/P(VDF-TrFE) heterostructure based highly sensitive and flexible pressure sensor *ACS Appl. Mater. Interfaces* **11** 16006–17
[31] Mun J, Kim Y, Kang I-S, Lim S K, Lee S J, Kim J W, Park H M, Kim T and Kang S-W 2016 Low-temperature growth of layered molybdenum disulphide with controlled clusters *Sci. Rep.* **6** 21854
[32] Kim T, Mun J, Park H, Joung D, Diware M, Won C, Park J, Jeong S-H and Kang S-W 2017 Wafer-scale production of highly uniform two-dimensional MoS_2 by metal-organic chemical vapor deposition *Nanotechnology* **28** 18LT01
[33] Mun J *et al* 2019 High-mobility MoS_2 directly grown on polymer substrate with kinetics-controlled metal–organic chemical vapor deposition *ACS Appl. Electron. Mater.* **1** 608–16